URDC

UTAH RESEARCH & DEVELOPMENT CO.

UTAH RESEARCH & DEVELOPMENT CO., INC.

SALT LAKE CITY, UTAH

Subsidiary of Interstate Engineering Corporation, Anaheim, California

P

THEORETICAL AND EXPERIMENTAL STUDY
OF
LOW VELOCITY PENETRATION PHENOMENA

SEMIANNUAL REPORT
Phases III, IV and V

Contract DA 19-129-AMC-150(X)

May 1965

Utah Research & Development Co., Inc.
1820 South Industrial Road
Salt Lake City, Utah 84104

Phone: (801) 486-1301

TABLE OF CONTENTS

Page

SUMMARY

A study of the strength of materials under large deformation has been conducted. The sample to be tested was in the form of a thin disk and was crushed between a fixed and a moving anvil. Velocities ranging from 10^{-3} to 10^4 cm/sec were obtained by driving the anvil either by a testing machine or by a compressed-air gun.

A simplified analysis of the problem is given, and the assumptions used are discussed and compared with the experimental data. The relationship between internal energy of the material and deformation is found to be $U = \mathcal{T} \ln (z_0/z)$ where U is energy per unit mass, z_0 and z are initial and final thickness of the disk and $\mathcal{T}$ is a constant, the "strength" of the material. Variations in $\mathcal{T}$ are discussed in terms of strain-rate effects and strain-hardening effects.

The materials tested were copper, 99.99 per cent pure aluminum, 6061-T4 and -T6 aluminum, Nylon, Lexan, Teflon, polyethylene and polypropylene.

1. INTRODUCTION

The purpose of research done under this contract is to develop a theoretical and experimental basis for predicting the behavior of materials under impact. The materials of interest range from simple, homogeneous materials such as metals or ceramics to complex structures made up of a variety of materials. Impact velocities of interest range from a few hundred to a few thousand feet per second.

One approach to solving the problem has been to develop a versatile computer program to solve the transient flow field for a general axisymmetric impact problem. Past work related to this has resulted in computer codes suitable for compressible inviscid fluids.[1] Work is in progress at several centers to include viscosity of the material in the program, but so far, only an artificial viscosity applicable to a Newtonian fluid has been used, and success is uncertain.[2]

In the velocity range of interest here, strength and plastic-flow effects are as important as inertial effects and probably dominate. For this reason, our approach has used elasticity and plasticity theory as well as a fluid-dynamics approach. Tensor formulation of finite-deformation problems has been explored to attempt to find the proper mathematical framework for the problem. A preliminary computer code has been developed for a simplified problem consisting of the edge-on impact of two finite-thickness sheets having infinite length and width. This work has been reported.[3]

A second approach to the general problem has been to formulate simple models of the impact process based on measurable dynamic material properties then to develop correlation formulae relating observed results to measured properties.

---

[1] R. L. Bjork, Effects of a Meteoroid Impact on Steel and Aluminum in Space, Technical Report P-1662, Rand Corp., Santa Monica, Calif., Dec. 16, 1958.

[2] T. D. Riney, "Visco-Plastic Solution of Hypervelocity Impact Cratering Phenomena," Proc. of Sixth Symposium on Hypervelocity Impact, Vol. II, p. 105, Firestone Rubber Co., Contract DA 31-124-ARO(D)-16, Cleveland, Ohio, Aug. 1963.

[3] Technical Reports on Contract DA 19-129-AMC-150(X), Final Report on Phases I and II, 28 June 1964, Semiannual Report, Phases III, IV, and V, November 1964.

In this report period, the work has been aimed at devising and analyzing a suitable experiment for measuring material strength under large deformation or flow. This information is essential for progress to be made in theory or for empirical comparisons of materials. The experiment chosen is that of crushing a disk between two moving rigid anvils. Reasonable simplifying assumptions make an analysis possible, and the necessary experimental measurements can be made. The results of this work are the subject of this report.

2. DISK-CRUSHING EXPERIMENT

The disk-crushing experiment uses two hardened-steel anvils, one fixed and one driven by a testing machine or shot from a gun. The disk is placed on the fixed anvil and some lubricant used to reduce friction. If a relatively thin disk is crushed between two unyielding anvils at a velocity which is low compared with wave velocity in the material, we may assume that the material is incompressible, inelastic, and that flow is laminar without friction with the anvils. With unyielding anvils and no stored elastic energy, the energy of crushing can be determined by measuring the testing machine force and travel distance or by measuring velocity and mass of the anvil shot from a gun. The time history of the deformation can be determined as well as the total energy involved. In practice, the assumptions prove to be justified or corrections can be made over limited ranges of the variables. The analysis of the problem and experimental procedures and results will be given in the following sections.

2.1 Differential Equations of Disk-Crushing

The geometry of the problem is as shown.
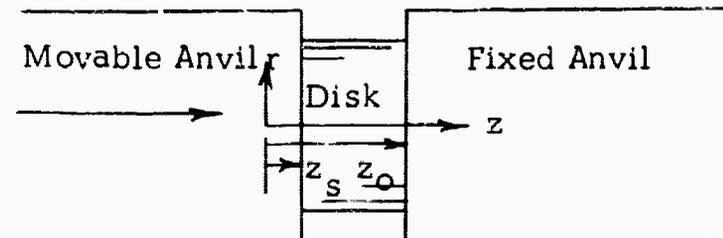
The subscripts used are as follows: o = initial condition, f = final condition, s = measurement made at the moving surface.

Neglecting body forces, the equations of continuity, motion, and energy for the system may be written in cylindrical coordinates as follows:

Continuity

$$\frac{\partial \rho}{\partial t} + \frac{1}{r}\frac{\partial}{\partial r}(\rho r v_r) + \frac{1}{r}\frac{\partial}{\partial \theta}(\rho v_\theta) + \frac{\partial}{\partial z}(\rho v_z) = 0 \qquad (1)$$

-3-

<u>Motion</u> (r component)

$$\rho\left(\frac{\partial v_r}{\partial t} + v_r \frac{\partial v_r}{\partial r} + \frac{v_\theta}{r} \frac{\partial v_r}{\partial \theta} - \frac{v_\theta^2}{r} + v_z \frac{\partial v_r}{\partial z}\right) = \tag{2}$$

$$-\frac{\partial \rho}{\partial r} - \left[\frac{1}{r} \frac{\partial}{\partial r}\left(r \tau_{rr}\right) + \frac{1}{r} \frac{\partial \tau_{r\theta}}{\partial \theta} - \frac{\tau_{\theta\theta}}{r} + \frac{\partial \tau_{rz}}{\partial z}\right]$$

(θ component)

$$\rho\left(\frac{\partial v_\theta}{\partial t} + v_r \frac{\partial v_\theta}{\partial r} + \frac{v_\theta}{r} \frac{\partial v_\theta}{\partial \theta} + \frac{v_r v_\theta}{r} + v_z \frac{\partial v_\theta}{\partial z}\right) = \tag{3}$$

$$-\frac{1}{r} \frac{\partial p}{\partial \theta} - \left[\frac{1}{r^2} \frac{\partial}{\partial r}\left(r^2 \tau_{r\theta}\right) + \frac{1}{r} \frac{\partial \tau_{\theta\theta}}{\partial \theta} + \frac{\partial \tau_{\theta z}}{\partial z}\right]$$

(z component)

$$\rho\left(\frac{\partial v_z}{\partial z} + v_r \frac{\partial v_z}{\partial r} + \frac{v_\theta}{r} \frac{\partial v_z}{\partial \theta} + v_z \frac{\partial v_z}{\partial z}\right) = \tag{4}$$

$$-\frac{\partial p}{\partial z} - \left[\frac{1}{r} \frac{\partial}{\partial r}\left(r \tau_{rz}\right) + \frac{1}{r} \frac{\partial \tau_{\theta z}}{\partial \theta} + \frac{\partial \tau_{zz}}{\partial z}\right]$$

The τ terms are the components of the stress tensor.

<u>Internal Energy U</u>

$$\rho \frac{DU}{Dt} = \rho\left(\frac{\partial U}{\partial z} + v_r \frac{\partial U}{\partial r} + \frac{v_\theta}{r} \frac{\partial U}{\partial \theta} + v_z \frac{\partial U}{\partial z}\right) =$$

$$-\left(\frac{1}{r} \frac{\partial}{\partial r}\left(r q_r\right) + \frac{1}{r} \frac{\partial q_\theta}{\partial \theta} + \frac{\partial q_z}{\partial z}\right) - p\left[\frac{1}{r} \frac{\partial}{\partial r}\left(r v_r\right) + \frac{1}{r} \frac{\partial v_\theta}{\partial \theta} + \frac{\partial v_z}{\partial z}\right]$$

$$-\left[\tau_{rr} \frac{\partial v_r}{\partial r} + \tau_{\theta\theta}\left(\frac{1}{r} \frac{\partial v_\theta}{\partial \theta} + \frac{v_r}{r}\right) + \tau_{zz} \frac{\partial v_z}{\partial z}\right] \tag{5}$$

$$-\tau_{r\theta}\left[r \frac{\partial}{\partial r}\left(\frac{v_\theta}{r}\right) + \frac{1}{r} \frac{\partial v_r}{\partial \theta}\right] \tau_{\theta z}\left(\frac{1}{r} \frac{\partial v_z}{\partial \theta} + \frac{\partial v_\theta}{\partial z}\right) - \tau_{rz}\left(\frac{\partial v_z}{\partial r} + \frac{\partial v_r}{\partial z}\right)$$

These equations may be simplified by the symmetry of the problem and by the assumptions mentioned.

One simple flow pattern assumes that the z velocity decreases linearly from that at the moving anvil to zero at the fixed anvil. We assume $\partial p/\partial z = 0$ during the time of interest after the first waves have passed through the disk. If the material is incompressible, the radial flow is then determined. The rate at which the piston displaces material at a portion of the circular disk of radius r is equal to the rate at which material flows out through the curved sides of the cylinder at r.

$$\pi r^2 v_s = 2 \pi r \left(z_0 - z_s \right) v_r$$

$$v_r = \frac{r \, v_s}{2 \left(z_0 - z_s \right)} \tag{6}$$

$$v_z = \frac{v_s \left(z_0 - z \right)}{\left(z_0 - z_s \right)} \qquad z_0 \geq z \geq z_s \tag{7}$$

v_s is a function of time and describes the motion of the moving anvil.

By symmetry $\dfrac{\partial}{\partial \theta} = 0$, $v_\theta = 0$, $\tau_{r\theta} = 0$, $\tau_{z\theta} = 0$

The continuity equation (1), becomes

$$\frac{\partial v_r}{\partial r} + \frac{v_r}{r} + \frac{\partial v_z}{\partial z} = 0 \tag{8}$$

Equations (6) and (7) satisfy this continuity equation.

The θ component equation of motion is identically zero.

The r and z component equations become:

$$\rho \left(\frac{\partial v_r}{\partial t} + v_r \frac{\partial v_r}{\partial r} \right) = -\frac{\partial p}{\partial r} - \left[\frac{\partial \tau_{rr}}{\partial r} + \frac{\tau_{rr}}{r} - \frac{\tau_{\theta\theta}}{r} \right] \tag{9}$$

-5-

$$\rho\left(\frac{\partial v_z}{\partial t} + v_z \frac{\partial v_z}{\partial z}\right) = -\frac{\partial \tau_{zz}}{\partial z} \qquad (10)$$

Considering these equations with (6) and (7), we see that by observing the dynamic deformation, v_s and $z_0 - z_s$, we can make important deductions as to material properties. By the assumed flow, relative material motion in the z direction is uniform throughout the disk, so $\partial \tau_{zz}/\partial z = 0$ v_z and v_r can then be determined by observing v_s and z_s. Some preliminary work in analyzing the equations of motion is reported in the experimental section.

In the energy equation, the pressure term is zero, as is seen by substituting Equations (6) and (7) into it. This is a result of the assumption of incompressibility. Heat transfer is neglected so the q terms are zero. The energy equation then becomes

$$\rho \frac{DU}{Dt} = \rho \frac{\partial U}{\partial t} + \rho v_r \frac{\partial U}{\partial r} + \rho v_z \frac{\partial U}{\partial z} =$$

$$-\left(\tau_{rr} \frac{\partial v_r}{\partial r} + \tau_{\theta\theta} \frac{v_r}{r} + \tau_{zz} \frac{\partial v_z}{\partial z}\right) \qquad (11)$$

This equation can be simplified further by using Equations (6) and (7).

$$\rho \frac{DU}{Dt} = -\frac{v_s}{z_o - z_s}\left(\frac{\tau_{rr}}{2} + \frac{\tau_{\theta\theta}}{2} + \tau_{zz}\right) \qquad (12)$$

Note that τ_{zz} is opposite in sign to τ_{rr} and $\tau_{\theta\theta}$ and $\partial v_z/\partial z$ is opposite to $\partial v_r/\partial r$ and v_r/r. The term in parenthesis may be lumped into one strength term τ.

Equation (12) provides a means of measuring τ and also τ_{rr}, $\tau_{\theta\theta}$ and τ_{zz} since when the material is deforming to a large degree, the three terms are probably about equal.

At low impact velocities, the strain is dominated by the dissipative τ term and is probably fairly uniform throughout the material. Under the assumptions, the dissipation is uniform throughout the disk so the substantial derivative can be replaced by dU/dt. Thus, the energy equation is of the simple form

-6-

$$\rho \frac{dU}{dt} = -\frac{\tau}{(z_0 - z_s)} \frac{dz_s}{dt}$$

For τ constant,

$$\rho U = \tau \ln \frac{z_0}{z_f} \qquad (13)$$

where z_0 and z_f are initial and final thickness of the disk.

The actual nature of τ can be investigated by measuring deviations from Equation (13) as strain rate or total strain is changed. Various useful approximate equations can be written based on experimental evidence. As an example, τ may be written with terms giving the strain-rate effect, the work-hardening effect and possible work softening effects.

$$\tau = a + b\left(1 - e^{-\frac{\dot{z}/z}{c}}\right) + d\left(1 - e^{-\frac{U}{f}}\right) + g\left(1 + e^{-\frac{U}{h}}\right) \quad (14)$$

The a coefficient is determined by static strength, the b term is determined by the magnitude of the strain-rate effect while c determines the strain-rate at which the effect becomes significant. Similarly, d and f determine the work-hardening effect depending on total energy dissipated or U and g and h represent a work-softening effect which dominates at higher energies.

The functional relationship among these variables may be quite different from that indicated here for some materials and some impact conditions. Under the brief exploratory program conducted so far, using copper, aluminum, and some plastics, the ideas embodied in Equation (14) seem adequate since τ is only weakly dependent on strain or strain rate and the constant term, a, dominates.

The experimental difficulties of separating friction effects from strain-hardening effects make the determination of d and f difficult.

One approach to correcting for friction uses the following model. An infinitesimal area $2\pi r\, dr$ on the disk at radius r from the center moves with velocity $r\, v_s/2(z_0-z_s)$. The power going into heat due to friction on this area is

$$P_f = \frac{F\, C_f\, \pi\, r^2\, v_s\, dr}{z_0 - z_s}$$

-7-

where F is the force per unit area under the test conditions and C_f is the coefficient of friction. Integrating from $r = 0$ to the outer radius R and multiplying by 2 to include both faces of the disk, gives the total power going into friction as

$$P_f = \frac{2 F C_f \pi v_s R^3}{3 (z_o - z_s)}$$

$v_s/(z_o - z_s)$ can be expressed in terms of R using Equation (6); P_f then becomes

$$P_f = \frac{4}{3} F C_f \pi v_r R^2$$

or

$$a W = \frac{4}{3} F C_f \pi R^2 dR$$

where W is the frictional energy. Integrating from initial to final disk radius

$$W = \frac{4}{9} F C_f \pi \left(R^3 - R_o^3 \right) \tag{15}$$

Disk mass is proportional to R^3 for disks of the same relative dimensions, so energy per unit mass contributed by friction is independent of disk size for disks of the same relative length to diameter.

Experiments have been conducted in a testing machine in which a disk is compressed in stages and comparisons made with new disks (not work hardened) corresponding to each of the stages. These tests clearly show the separation of effects of work hardening and friction but have not yet been analyzed to obtain quantitative values for the coefficients in Equations (14) and (15).

2.2 Experimental Work

Disks made of copper, aluminum, and various plastics have been deformed by two methods: (1) by impacting them at velocities of ten to seventy meters per second with a hardened-steel cylinder, and (2) by compressing them in a testing machine under static conditions. The deformation rate in experiments using these two methods varied by as much as a factor of 10^7. It was anticipated that such a variation would show any strain-rate dependency in the materials tested merely by observing variations in T using Equation (13).

Most of the disks were of the same original size; 1/4 inch diameter by 1/8 inch thick. However, copper disks of other sizes were also used. Materials used were annealed and unannealed copper, 99.99 per cent pure aluminum, 6061-T4 and 6061-T6 aluminum alloy, Nylon, Lexan, Teflon, polyethylene and polypropylene.

The specific energy (energy per gram of material) and the degree of deformation (the ratio of the final disk thickness to its original thickness) have been determined for each impact shot and for each compression test. In Figures 1 to 7, deformation is plotted on a logarithmic scale versus specific energy. Figure 1 shows data for copper, Figure 2 shows data for aluminum, and Figures 3 to 7 show data for plastics. If the relationship expressed in Equation (13) is correct, lines drawn through the points in these figures will be straight, indicating that specific energy is directly proportional to the logarithm of the final and original disk thickness ratio. This is seen to be approximately true for all cases.

In Figure 1, the data for copper show that there is no observable difference between disks of different sizes. This indicates that friction losses are proportional to mass for disks of the same relative dimensions. The best-fit curves to the copper data are shown in Figure 8. Data points are omitted for clarity. Differences are shown in Figure 8 between annealed and unannealed copper, indicating strain-hardening effects and between static and impact data, indicating strain-rate effects.

The data for aluminum in Figure 2 show some effects of friction or strain hardening and show a large strain-rate effect. This is shown by the difference in position of the data points from static and impact tests.

In Figures 3 to 7, both static and dynamic data concerning five different plastics are shown. In each one, a strong rate dependency is exhibited showing that it is stronger under impact conditions than under static conditions. It is also shown that under impact conditions, an apparent "strain-softening" effect exists for Nylon and polypropylene.

A quantitative analysis of these data has not yet been made to determine the coefficients in Equation (14) or the coefficient of friction of Equation (15).

2.3 Dynamic Measurements

An experimental arrangement for measuring the motion of the disk being crushed is shown in Figure 9.
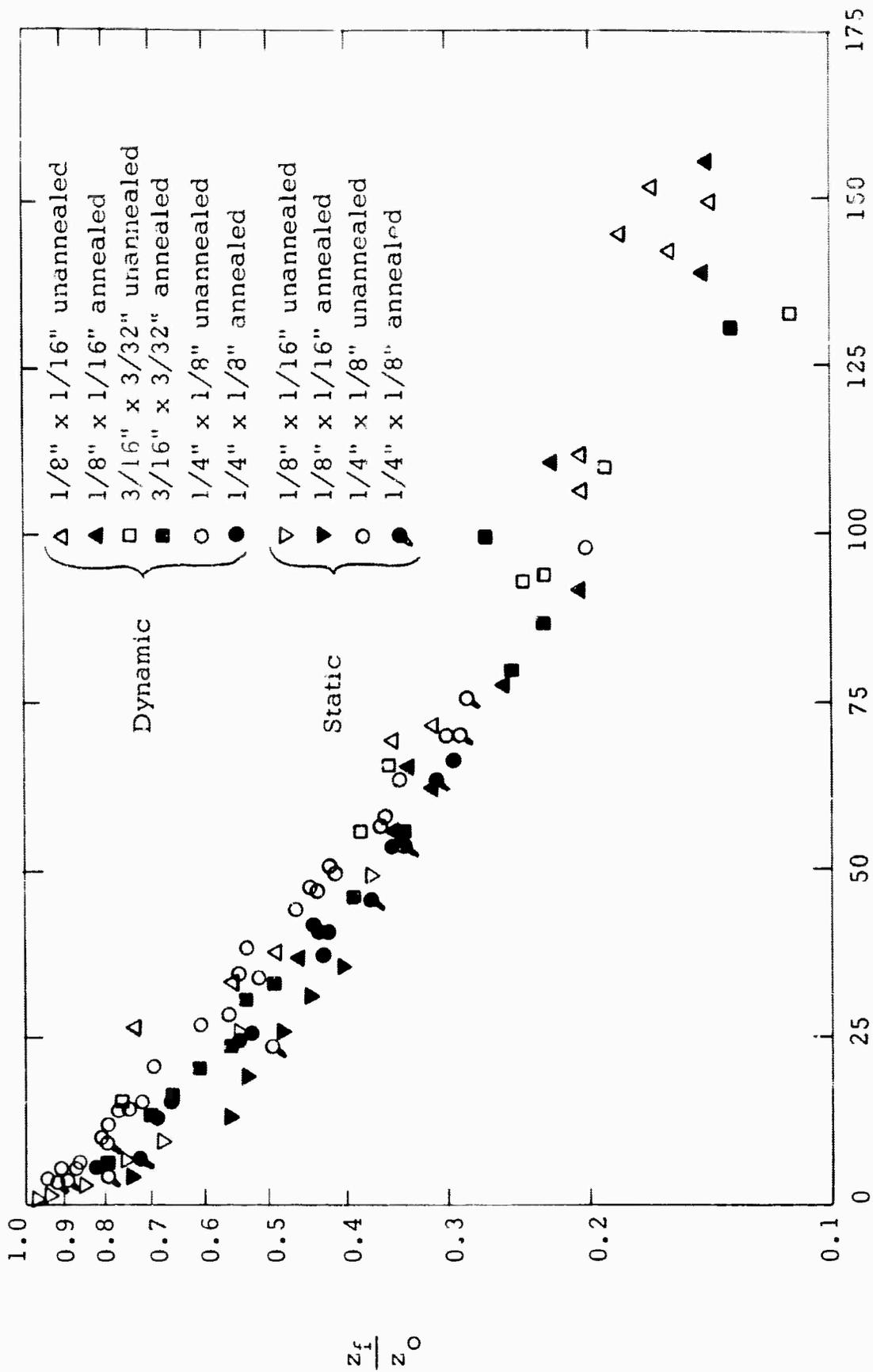
FIGURE 1. Copper

(See Figure 8 for separate curves for these data.)

Specific Energy of Disk Material, E_{sp} (Joules/gram)

$\dfrac{z_f}{z_o}$

● 99.99% pure, shear strength = 9,550 psi ⎫ Static
○ 99.99% pure, shear strength = 9,550 psi ⎫
△ 6061-T4, shear strength = 24,100 psi ⎬ Dynamic
□ 6061-T6, shear strength = 31,600 psi ⎭
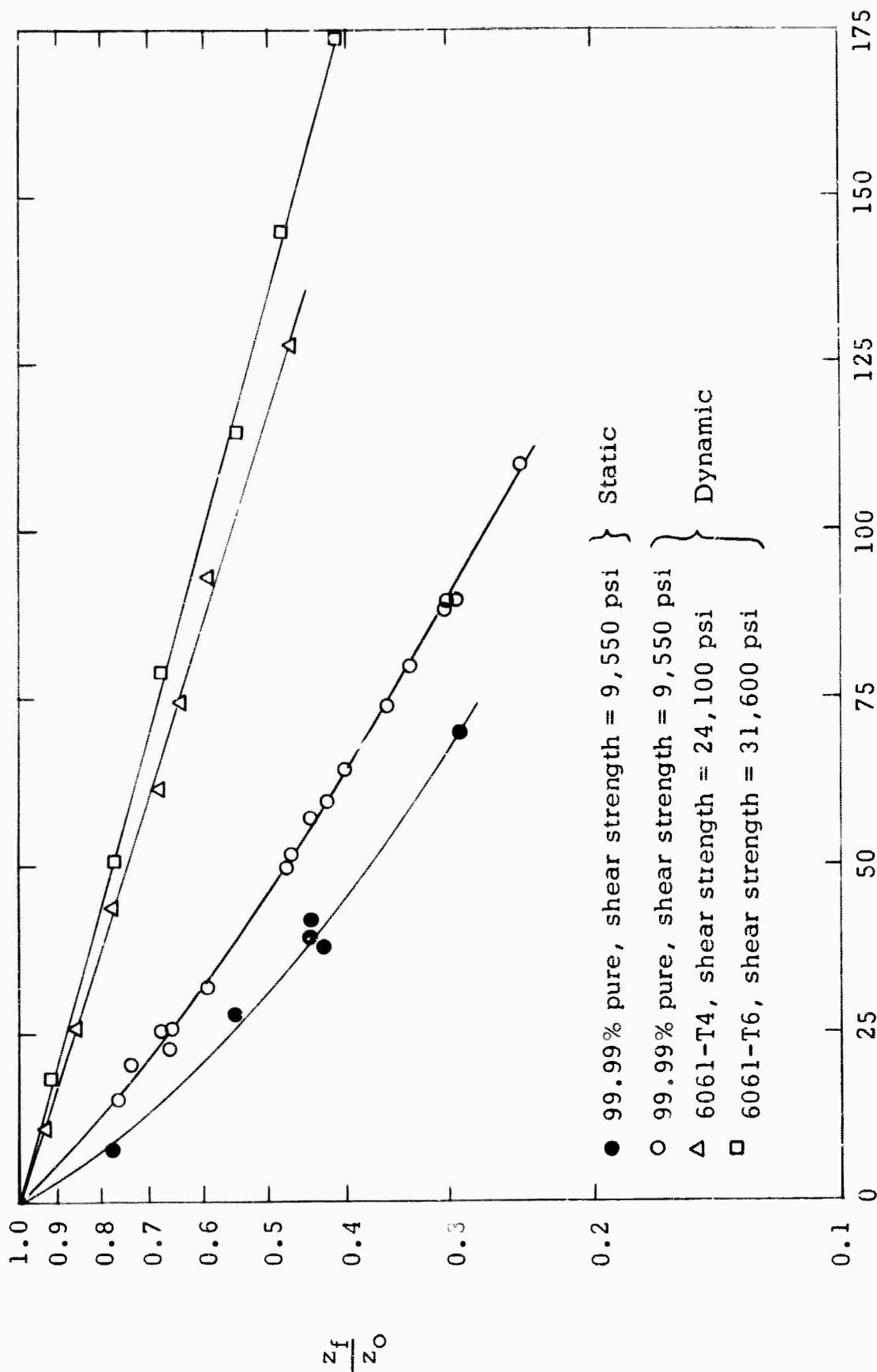
FIGURE 2. Aluminum
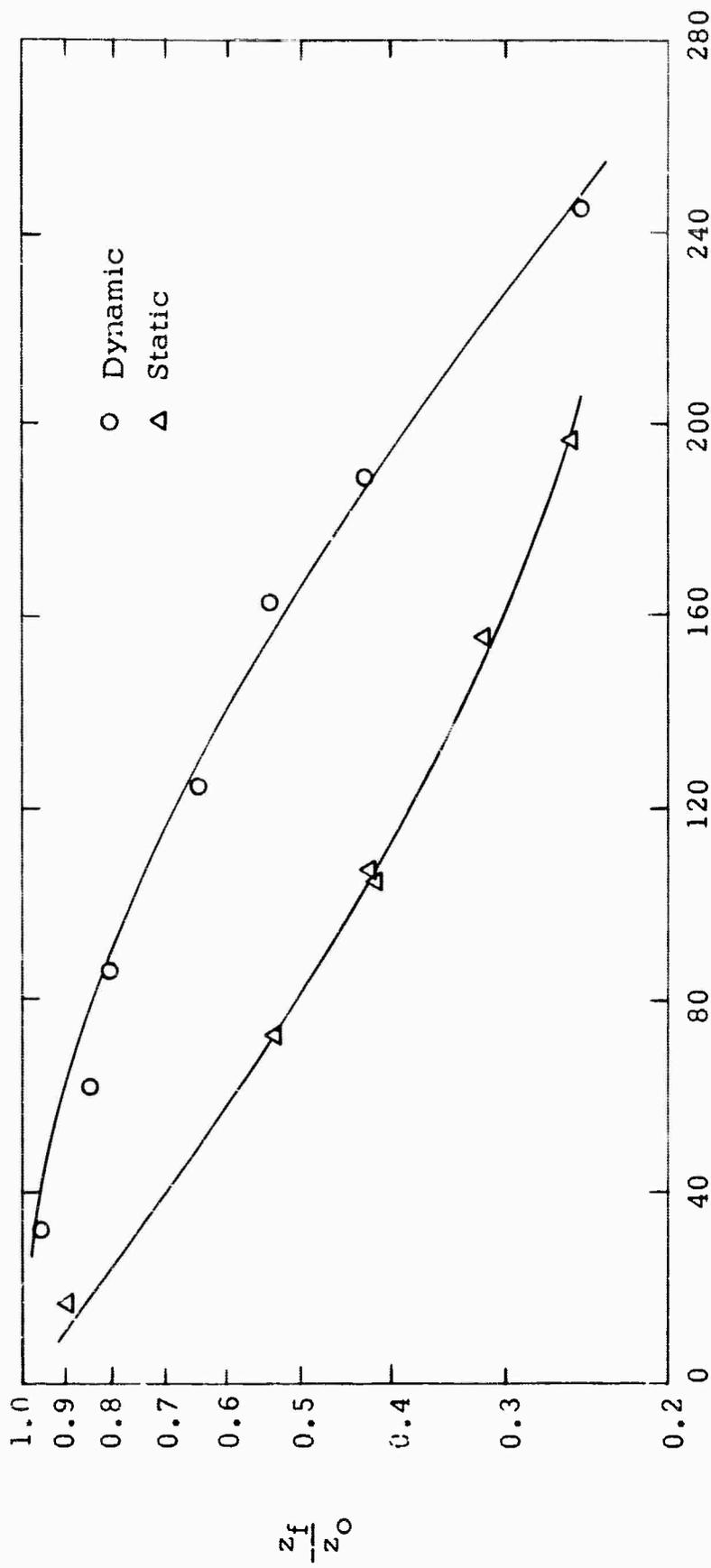
Specific Energy of Disk Material, E_{sp} (Joules/gram)

FIGURE 3. Nylon

○ Dynamic

△ Static

$\dfrac{z_f}{z_o}$

Specific Energy of Disk Material, E_{sp} (Joules/gram)
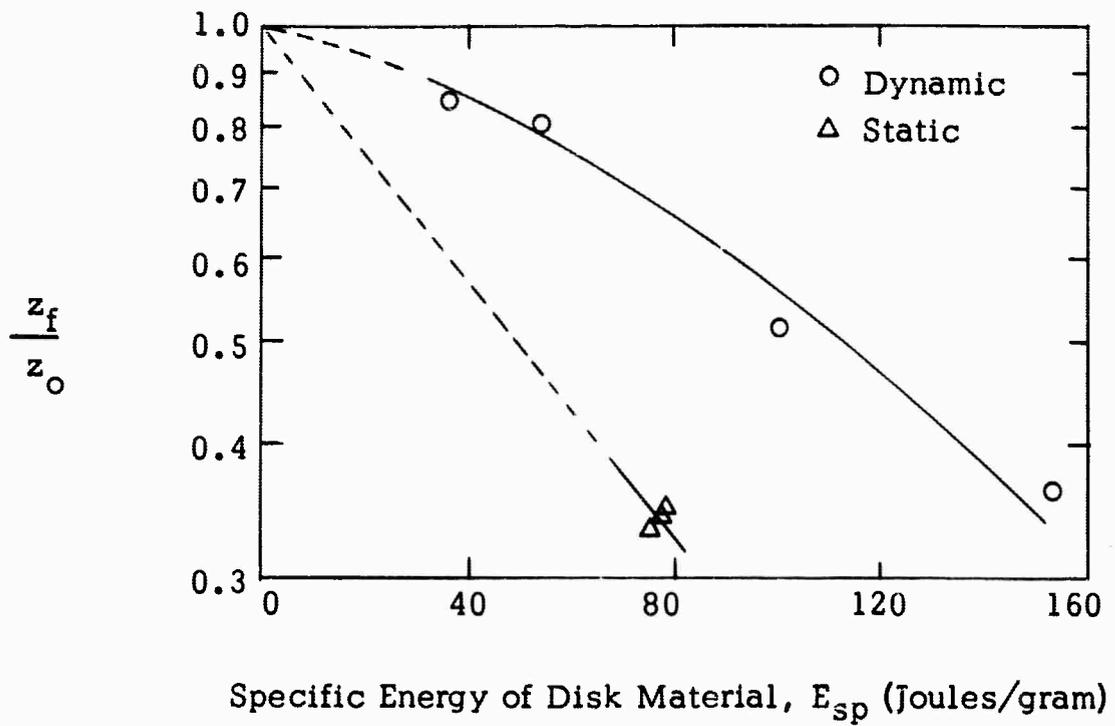
FIGURE 4.   Polypropylene

Specific Energy of Disk Material, E_{sp} (Joules/gram)

FIGURE 5.   Lexan

-13-
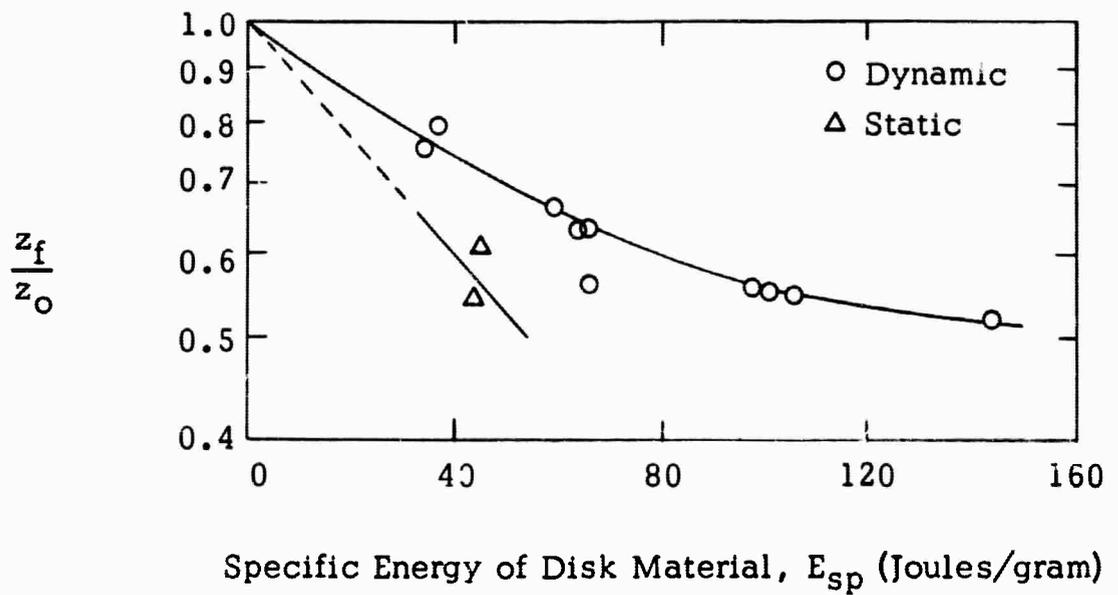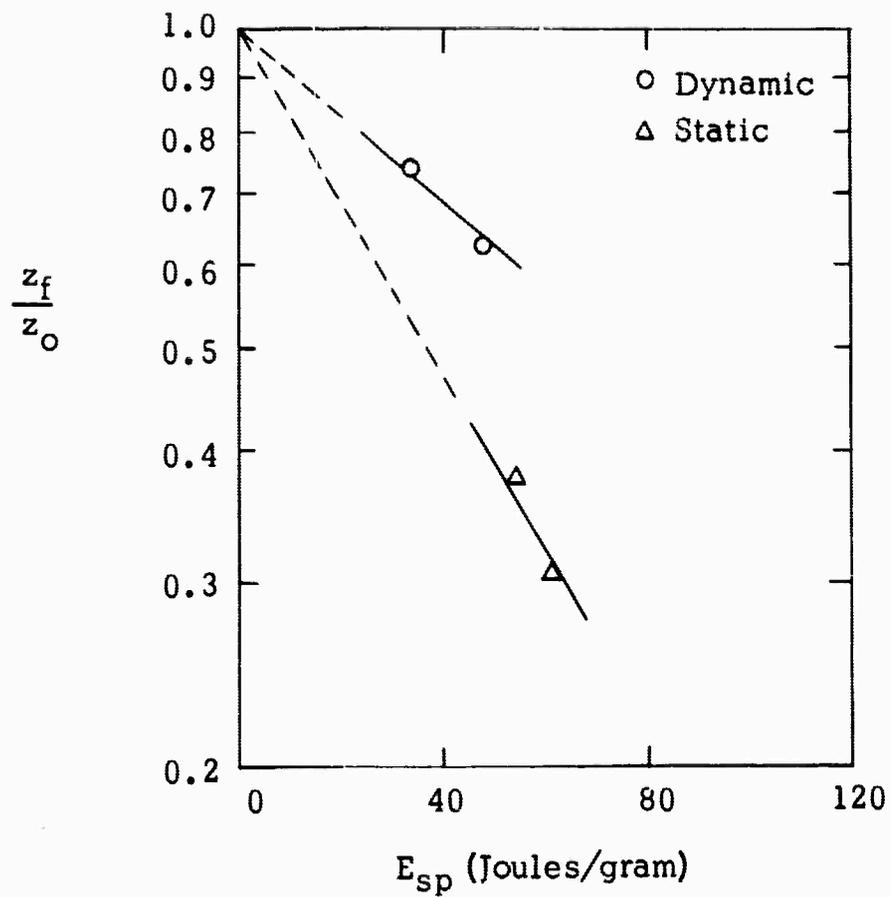
FIGURE 6.   Polyethylene
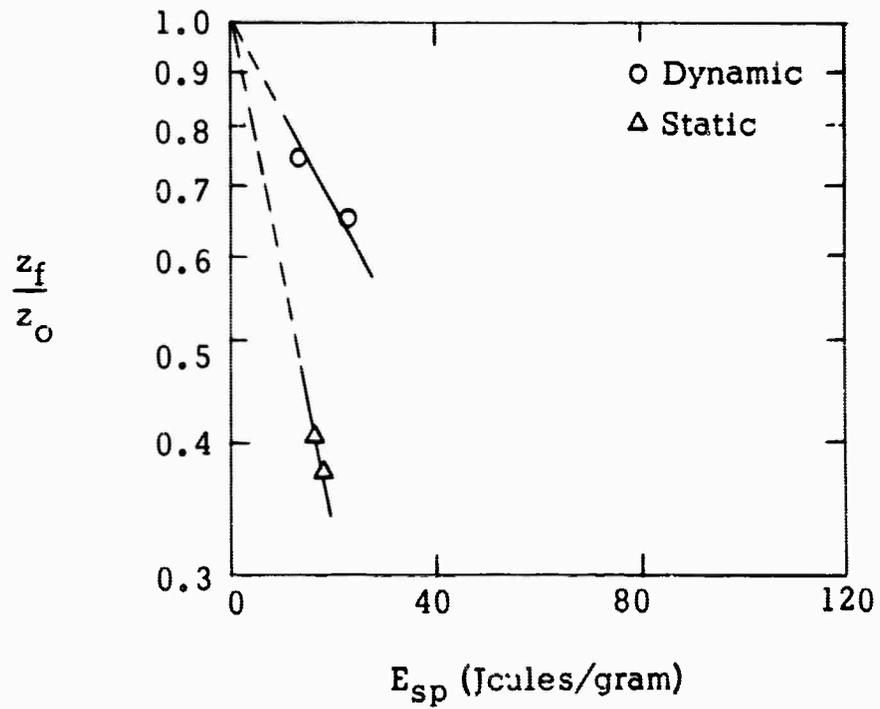
FIGURE 7.   Teflon
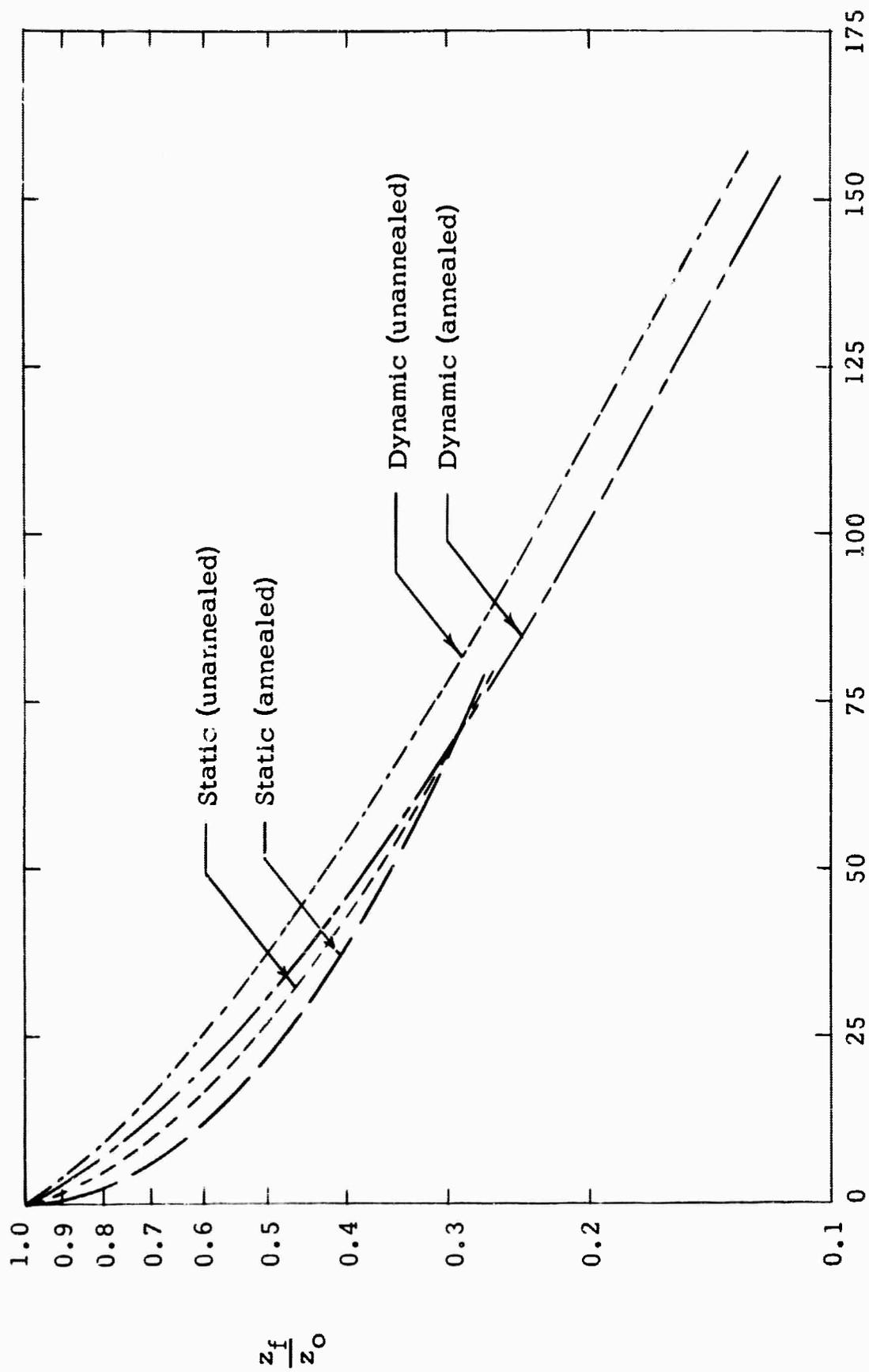
FIGURE 8. Best-fit Curves Through the Data of Figure 1. Strain-rate Effect is Shown by the Displacement Between Comparable Static and Dynamic Curves.

Side View of Anvils and Disk

Top View Showing Optics
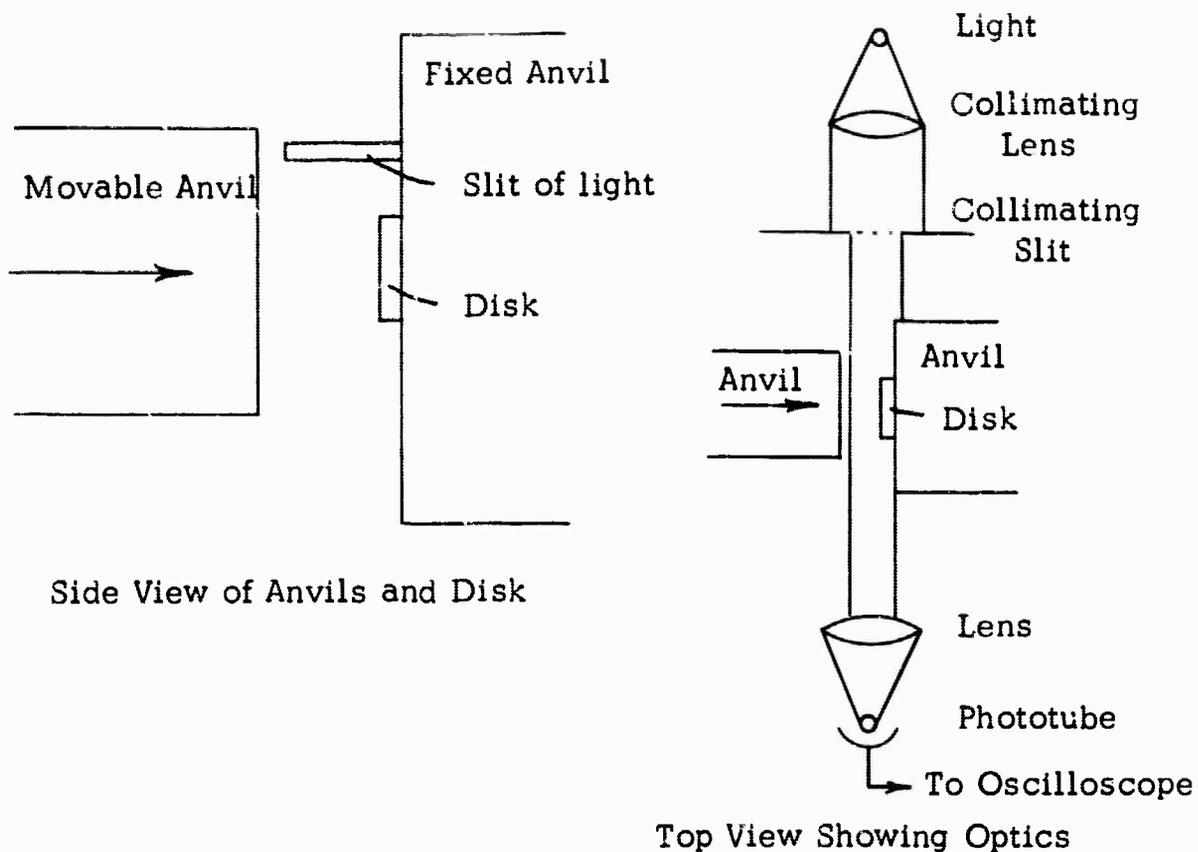
FIGURE 9. Experimental Arrangement for Measuring Displacement
and Velocity of Moving Anvil.

An oscillogram of the light intensity, which is proportional to distance of
separation of anvils, and the differential of this signal, which is proportional
to velocity, v_s, is shown in Figure 10.
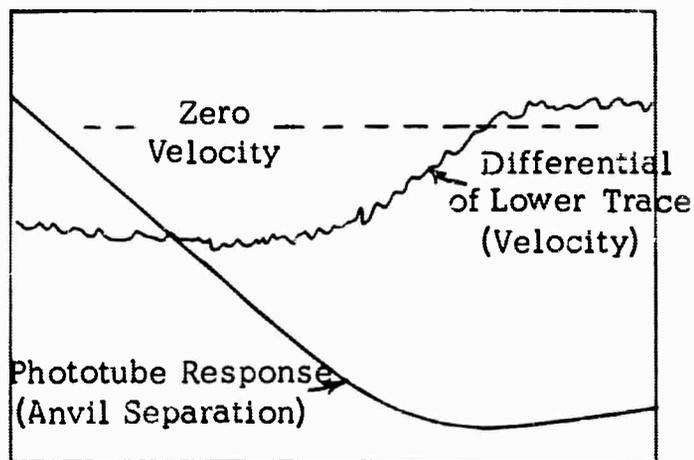
FIGURE 10. Displacement and Velocity of the Moving Anvil
of Figure 9.

-16-

A plot of the acceleration, obtained by graphical differentiation of the displacement and velocity curves, is shown in Figure 11. The data for this shot are given in Table I.

The energy going into the disk, computed from the dynamic data, agrees closely with that obtained from measurements of rod velocity and mass. The low rebound velocity of the rod indicates that less than 5 per cent of the kinetic energy of the rod goes into recoverable elastic energy of anvils and disk at these impact velocities.

Data for a similar shot at higher velocity are shown in Table II.

A rough estimate of the ratio of power going into the acceleration of material to that being dissipated in the material is given by comparing the rate of change of kinetic energy of the material with the rate of change of internal energy. These energies are plotted in Figure 12 for the data of Table I. Note the different scales for internal energy and kinetic energy. The maximum slopes indicate that the maximum power going into internal energy is 60 times that going into kinetic energy. Impact velocity would have to go up from 3.52 x 10^3 cm/sec to about 2.8 x 10^4 cm/sec for power going into kinetic energy to equal that going into internal. Unfortunately, tests cannot be made to see how internal energy behaves at this impact velocity since the disk would be so thin that friction with the anvil faces would dominate the process; also the anvils could not be considered rigid.

As yet, the dynamic measurements have been used only to compare integrated power data with total impact energy computed from rod velocity and mass and to compare instantaneous pressure with static testing-machine pressure data. No effort has been made to find the time function which satisfies the equations of motion. It is interesting to note that the maximum pressures indicated by the two dynamic shots are 7.9 x 10^9 and 8.6 x 10^9 dyne/cm^2. The agreement between these two shots at different velocities allows a good estimate to be made of the strength of copper under flow conditions. A disk pressed to similar thickness in a testing machine shows higher pressure, about 12 x 10^9 dyne/cm^2. The machine-tested disks were barrel shaped after compression while those tested at high velocity were nearly right cylinders with straight sides. This probably indicates greater friction in the testing machine.
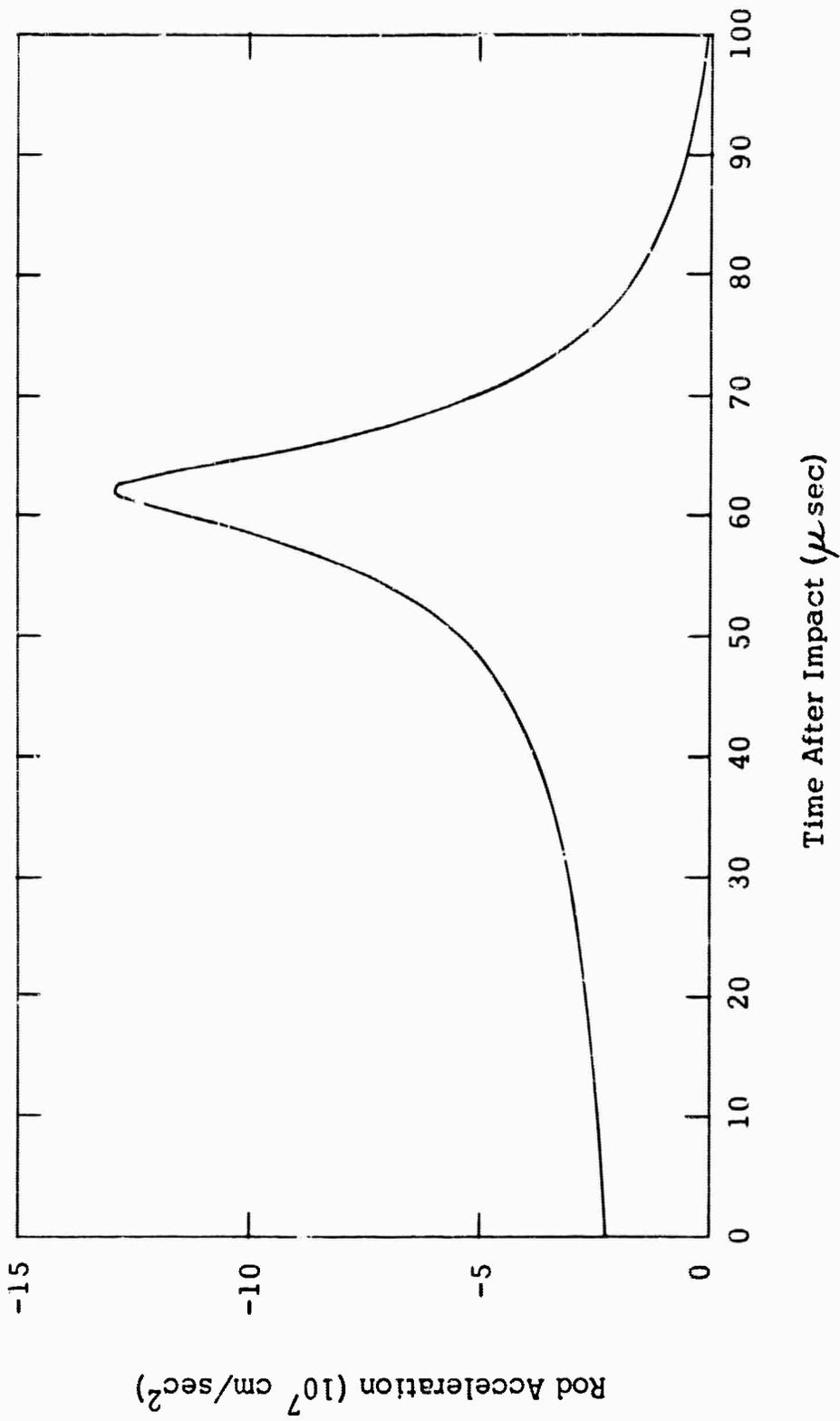
FIGURE 11. Acceleration of the Moving-rod Anvil as a Function of Time

TABLE I

DATA FROM ROD-DISPLACEMENT MEASUREMENTS FOR IMPACT OF A HARDENED-STEEL ROD ON A COPPER DISK

Rod

Steel
1/2" diameter x 2" long
Mass = 49.9 g

Copper Disk

Initial Diameter	= .470 cm
Initial Thickness	= .213 cm
Final Diameter	= .290 cm
Final Thickness	= .048 cm
Mass	= 0.330 g

Rod velocity 3.52×10^3 cm/sec
Kinetic energy 30.9 Joule

Time After Impact (μsec)	Distance Moved After Impact (cm)	Disk Thickness (cm)	Disk Radius (cm)	Rod Velocity (10^3 cm/sec)	Rod Acceleration (10^7 cm/sec^2)	Axial Velocity Gradient (10^3cm/sec)/cm	Radial Velocity of Disk (10^3 cm/sec)
0	0	.213	.235	3.51	-2.2	16.5	1.94
8	.027	.186	.251	3.32	-2.4	17.8	2.24
16	.052	.161	.270	3.12	-2.2	19.3	2.61
24	.076	.137	.292	2.92	-2.8	21.3	3.08
32	.099	.114	.320	2.69	-3.2	23.4	3.72
40	.119	.094	.354	2.42	-3.8	25.8	4.48
48	.138	.075	.396	2.08	-4.9	27.8	5.43
56	.152	.061	.439	1.58	-8.2	25.9	6.19
64	.162	.051	.480	0.68	-11.4	13.3	6.03
72	.164	.049	.489	0.15	-4.0	3.1	3.09
76	.165	.048	.495	0	-2.5	0	0

TABLE I (Continued)

Time After Impact (μ sec)	Force (10^9 dyne)	Power (10^{12} erg/sec)	Integrated Energy (10^7 erg)	Pressure (10^9 dyne/cm^2)
0	1.10	3.86	0	6.33
8	1.20	3.98	3.12	6.06
16	1.30	4.05	6.28	5.67
24	1.40	4.08	9.51	5.22
32	1.60	4.30	12.89	4.96
40	1.90	4.60	16.44	4.82
48	2.44	5.08	20.28	4.95
56	4.09	6.46	24.75	6.75
64	5.68	3.86	29.50	7.85
72	2.00	.30	30.81	2.68
76	1.25	0	30.85	1.98

TABLE II

DATA FROM ROD-DISPLACEMENT MEASUREMENTS FOR IMPACT
OF A HARDENED-STEEL ROD ON A COPPER DISK

Rod

Steel
1/2" diameter x 2" long
Mass = 49.9 g

Copper Disk

Initial Thickness = 0.249 cm
Final Thickness = 0.026 cm
Change in Thickness = 0.223 cm

Impact velocity = 4.58×10^3 cm/s
Kinetic energy of projectile = 2.4 Joules

Time After Impact (μ sec)	Distance Traveled By Rod (cm)	Thickness of Disk (cm)	Disk Radius (cm)	Disk Area (cm^2)	Rod Velocity (10^3 cm/sec)	Rod Acceleration (10^7 cm/sec^2)	Velocity Gradient (10^4 cm/sec)/cm
0	0	.249	.237	.177	4.58	-0.464	1.84
8	.039	.208	.259	.210	4.50	-1.10	2.16
11	.048				4.58	-1.43	
16	.074	.171	.286	.257	4.40	-2.10	2.57
24	.108	.135	.322	.326	4.20	-3.30	3.11
31	.136				3.81	-5.33	
32	.140	.102	.370	.430	3.81	-5.10	3.74
40	.167	.073	.439	.606	3.32	-7.60	4.55
44						-9.16	
48	.190	.049	.534	.896	2.58	-12.70	5.26
51	.198				2.12	-16.9	
54	.204	.034	.643	1.30	1.57	-21.0	4.62
55	.206	.032	.660	1.37	1.25	-23.6	3.90
56	.206	.032	.660	1.37	1.15	-19.1	3.59
60	.209	.029	.694	1.51	0.61	-9.88	2.10
64	.211	.027	.720	1.63	0.30	-6.60	1.11
70	.212	.026	.734	1.69	0	-4.01	0

TABLE II (Continued)

| Time After Impact (μ sec)	Force (10^9 dyne)	Power (10^{12} erg/sec)	Pressure (10^9 dyne/cm^2)
0	.231	1.06	1.31
8	.548	2.46	2.61
11			
16	1.04	3.51	4.05
24	1.64	6.88	5.04
31			
32	2.54	9.69	5.40
40	3.78	12.6	6.23
44			
48	6.33	16.3	7.08
51	8.41	17.8	
54	10.5	16.5	8.09
55	11.78	14.7	8.60
56	9.51	10.9	6.95
60	4.92	3.00	3.26
64	3.29	0.987	2.02
70	2.00	0	1.18
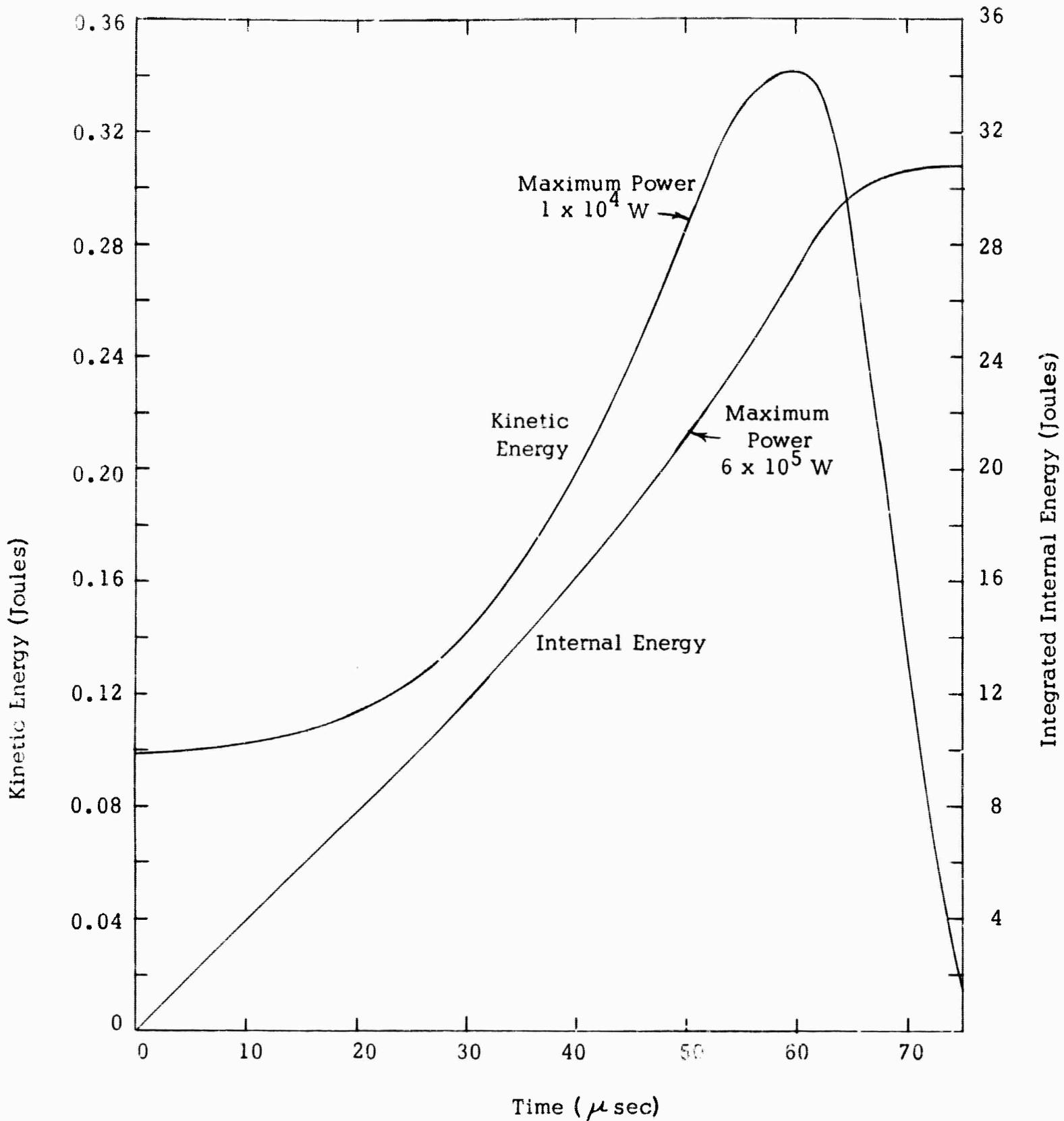
FIGURE 12. Kinetic Energy of Disk Material Compared with Internal Energy of Material for the Data of Table I.

3. CONCLUSIONS

The disk-crushing experiment gives quantitative measurements of the energy involved in the flow of solid materials and is useful where the material to be tested is less rigid than the anvils. The assumptions made in the simplified analysis are adequate for small deformations and can be corrected from the experimental results. Dynamic measurements can be made and the effects of strain rate and st ain hardening on the strength of materials can be determined.

These data allow an immediate means of comparing materials as to their resistance to flow deformation. They provide necessary data for any complete theoretical analysis of the impact problem.

4. FUTURE WORK

The disk-crushing experimental work will be extended somewhat. The plastics, which have strain-rate dependent strength, will be tested at intermediate strain rates using a gun or a drop tower. The strength of frangible materials, such as fiberglass-reinforced plastics or acrilics, will be tested using the dynamic methods described, since before-and-after measurements are not possible. The experiments on friction will be analyzed and extended. The purpose of these tests is to make quantitative measurements of the physical properties of materials under flow conditions and to express these properties by appropriate equations such as Equation (14).

Shear and tension properties will be measured by shooting through thin sheets or into wires of the material being tested. This is an extension of work reported previously. The relationships between deformation, energy dissipation in the material, and projectile energy loss will be determined.

The compression, shear and tension data will be used to formulate simplified mathematical models of the impact problem and to rate pure materials and composites as to their method of failure, the energy involved, and their ability to withstand penetration.

The computer program reported earlier will be simplified in an effort to obtain earlier limited results. The unique predictor-corrector scheme used previously will be developed further. The tensor analysis of deformation will be severely simplified and modified. The easily measured material properties coming from the disk-crushing experiment and from the tensile-failure tests will be used rather than a tensor formulation of material properties.